

FACTA UNIVERSITATIS

Series: **Electronics and Energetics** Vol. 28, N° 2, June 2015, pp. 263 - 274

DOI: 10.2298/FUEE1502263A

## DESIGN OF CMOS READOUT FRONTEND CIRCUIT FOR MEMS CAPACITIVE MICROPHONES

**Daniel Arbet, Viera Stopjaková, Martin Kováč, Lukáš Nagy,  
Gabriel Nagy**

Slovak University of Technology in Bratislava  
Faculty of Electrical Engineering and Information Technology  
Institute of Electronics and Photonics  
Department of IC Design and Test

**Abstract.** *This paper deals with a frontend part of the readout circuit developed as an integrated circuit that after bonding together with a MEMS capacitive microphone (MCM) chip will be used in a noise dosimeter applicable in very noisy and harsh environment, e.g. mine. Therefore, the main attention has been paid to the high dynamic range, low offset and low noise of the developed readout interface as well as its low-power consumption feature. For conversion of the MCM's capacitance variation into voltage, an approach based on the buffered input conversion stage biased by a voltage divider was used. The advantage of this approach is that the voltage divider formed by MOS transistors can be connected to the high-impedance node (i.e. the output of the MCM, in this case). The whole frontend part of the readout interface was designed in a standard 0.35 $\mu$ m CMOS technology. Finally, the achieved results are discussed and compared to other works.*

**Key words:** *readout interface, MEMS microphones, analog front-end, preamplifier*

### 1. INTRODUCTION

MEMS (Micro-Electro-Mechanical-System) microphones are commonly used devices in a portable electronic systems, because they offer the miniaturization and integration of the whole system on a single chip. For such integration, CMOS technology is rather advantageous thanks to its good compatibility with MEMS manufacturing process and relatively low price. MCMs are acoustic sensors being proposed to improve the integration and cost of acoustic systems by employing great features of advanced MEMS technologies. Even though the well-known Electret-Condenser-Microphones (ECM) still represent the current market solution for most of acoustic applications, MCMs are considered as the future choice for mobile phones, consumer electronics and number of medical applications,

---

Received August 29, 2014; received in revised form December 4, 2014

**Corresponding author:** Daniel Arbet

Department of IC Design and Test, Slovak University of Technology, Ilkovicova 3, 812 19 Bratislava, Slovakia  
(e-mail: daniel.arbet@stuba.sk)

e.g. hearing aids [1]. With the fast development of MEMS technologies also the field of possible applications for MEMS sensors is getting wider.

MCMs offer several advantages over the classical ECMs. First of all, they are smaller in size, compatible with high-temperature automated printed circuit board (PCB) mounting process and less susceptible to mechanical shocks. Furthermore, the possibility of monolithic integration of the sound sensor with CMOS electronics is another major advantage towards a robust and cost-effective system, enabling both the electrical and mechanical properties of silicon.

To convert the output of a MCM (capacity variations in order of fF-pF) into an appropriate electrical signal representation, dedicated circuitry, either analog or digital so-called readout interface is required [2]–[5]. This necessitates a low-noise signal conversion provided by the readout interface. Additionally, in recent applications, low-power profile is required in order to provide the system portability.

In our research, a MCM-based application specific integrated circuit (ASIC) designed as a part of a portable low-cost noise dosimeter for very noisy and harsh environment is targeted. Therefore, the main goal is to develop a novel readout circuit schemes suitable for such applications. Thus, the most significant features of the developed ASIC are: low power, low cost and mass production aspects. Moreover, a wide dynamic range of the developed analog frontend is one of the major priorities as well. Thus, this paper presents an approach based on the buffered conversion input stage biased by a voltage divider that is formed using diode-connected MOS transistors. A MOS transistor of small size exhibits high resistance and therefore, such a voltage divider can be connected to high impedance node i.e. the microphone output. This solution ensures reliable DC bias voltage for an input buffer of the readout circuit. Moreover, with high-resistance MOS transistors, low-frequency pole of the MCM with a small value of the nominal capacitance can be easily set.

## 2. PRELIMINARY WORK

Microphone is a device, which converts the sound into an electrical signal. Typical structure of a MEMS capacitive microphone is shown in Fig. 1. Acoustic sound pressure incident the diaphragm (membrane) causes capacitance changes of the structure that is then transformed into electrical signal by the readout circuit. The MCM has a diaphragm and cavity like some other MEMS microphones. However, compared to other types, MCMs have a fixed and porous backplate that is separated from the diaphragm by the air gap. The backplate holes are used to tune the bandwidth and resonance frequency of the microphone [6].

Generally, capacitive microphone can be classified as electret and condensed. Electret microphones are less used because they are biased with the stable embedded charge and therefore, the fabrication is more difficult. Condensed microphones are biased by an external voltage source, which makes them easier to use. Accordingly, the sensitivity of the capacitive microphone depends on the size of the membrane as well as on the electric field in the air gap that is invoked by the external voltage source [1].

### **Readout interface**

The main role of the readout interface (RI) is to convert the capacitance changes produced by an MCM into electrical signal such as voltage, current, etc. In the last years,

many readout circuits based on the capacitive sensing for MEMS sensors and its several modifications have been proposed [2,4,7-11].

The most important requirements for the MCMs readout interface include very high input impedance, low offset and low noise. On the other hand, the design of readout circuitry strongly depends on features of the MCM but it is also determined by the end application. Therefore, it is not easy to make the optimum design of the readout circuit, which could fulfill all the requirements.

In general, there are three basic approaches (based on a preamplifier) to readout circuit topology, depending on the method used for the microphone capacitance conversion. Those are: constant-voltage, constant-charge and force-feedback approaches [12].

In continuous time *constant-voltage approach*, changes in capacitance of the MCM caused by acoustic input pressure create an AC current that can be sensed using a preamplifier with extremely high input impedance so called transimpedance amplifier (TIA) [8]. In this approach, the microphone output node tries to be maintained fixed (termed as the DC-component of the sensor) that mitigates the influence of parasitic capacitances. This results in the transformation of charge change( $\Delta Q$ ) by a charge preamplifier into output voltage signal. The DC biasing of the preamplifier input in constant-voltage approach is not so critical, and also pole of high pass filter can be localized more properly [12, 17]. In [9], this approach was supported by floating-gate circuit techniques to adapt the charge and improve SNR.

Constant-voltage approach can be also implemented in the discrete form. Therefore, switched capacitor (SC) circuits can be also used to implement a readout circuit for the MCMs [2,8]. Using SC circuits, the robust DC bias in the sensing node can be achieved and the influence of the MCM parasitic capacitance can be reduced. Low input offset can be achieved by employing the offset reduction techniques used for SC circuits like auto-zero, correlated double sampling or chopper stabilization technique [18-20]. However, the main disadvantage of a SC readout circuit is thermal noise of the switches,  $kT/C$  noise caused by sampling capacitors as well as noise produced by sampling process itself.

Better noise performance can be achieved with *constant-charge approach* based on an impedance conversion buffer, where the capacitance change is converted into a voltage signal by proper biasing of the MCM. However, in this approach, high impedance of the preamplifier dramatically influences the frequency band and stray impedance of the MCM and also attenuates the microphone sensitivity. Nevertheless, the effect of interconnects and parasitic capacitances can be reduced by bootstrapping [12-13]. Preamplifier offset also belongs to critical features of this approach. Despite these disadvantages, constant-charge approach still remains popular [14-16]. However, the key challenge in this technique is setting the DC bias voltage at the MCM output (represents the very high impedance node). Approaches presented in [21-22] uses diodes and a unity gain OTA (Operational Transconductance Amplifier) for DC biasing and for current to voltage conversion.

*Force-feedback approach* has been commonly used to minimize the impact of mechanical imperfections and inherent non-linearities in MEMS capacitive sensors through close-loop bias voltage tuning [14, 23]. A feedback loop can be successfully exploited for offset cancellation and the dynamic range enhancement [24-25]. The reset noise reduction schemes [26] also include a feedback loop that either cancels the reset noise or reduces the bandwidth of noise or controls the reset process itself. Interesting concept was presented in [27], where electro-mechanic feedback incorporates a triangle voltage wave generator. In combination with the constant-voltage approach and transimpedance amplifier, high

dynamic range was achieved. However, the power consumption, sensitivity, a range of capacitance variation and lower limit of sense capacitance make this readout design impractical for MEMS microphones. This concept belongs to the semi-digital methods that encode the information either in time (pulse-width modulation) or frequency (pulse-frequency modulation) domain. Therefore, main advantages include broad dynamic range, low power consumption and robustness against the environmental noise. However, the vast majority of realizations do not meet the readout circuit requirements for MEMS microphones[22-27].

This paper presents a novel constant-charge approach, where the voltage divider based on diode-connected MOS transistor is used for DC biasing of the input conversion LNA (Low Noise Amplifier) buffer. Advantage of this approach is that the high-resistance voltage divider does not affect the high output impedance of the MCM, and also the pole of high pass filter can be easily localized.

### 3. PROPOSED READOUT FRONTEND CIRCUIT

#### 3.1. The whole RI concept

The principal scheme of the proposed RI is shown in Fig. 1. The proposed readout approach is based on the buffered conversion input stage. Whole RI was designed in a standard 0.35  $\mu\text{m}$  CMOS technology, with the supply voltage of 3V. Generally, the readout interface for MCMs can be divided into two main parts - frontend part and backend section. In our case, the frontend part consists of the impedance conversion buffer (input conversion block), preamplifier and filters while the sigma-delta modulator, which converts the output of the frontend circuitry into a digital form, represents the backend part of the RI.

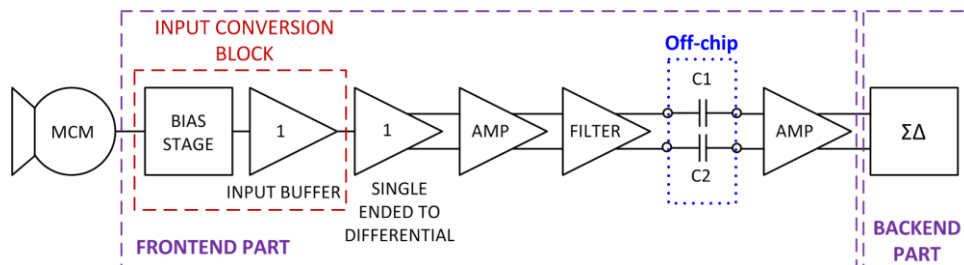


**Fig. 1** Concept of the proposed RI

In this paper, we present the frontend part of the proposed RI. Because of high output impedance of the MCM, a buffer with low output impedance has been connected to the microphone's output. Capacitance variation at the MCM output is converted into voltage using so-called sensing element that is followed by the input buffer. The sensing element has been also used to ensure the DC bias voltage for the input buffer. In general, the input buffer can be implemented using a source follower, a common-gate amplifier or an operational amplifier (OPAMP) based voltage follower. In our case, a simple two stage OPAMP connected as a voltage follower was used.

Usually, the sensing element requires high resistance and therefore, it is implemented by a diode-connected MOS transistor or by a diode in the reverse direction. The sensing element is the most critical part of the RI because several significant parameters (e.g. sensitivity, low corner frequency, DC bias voltage, etc.) of the microphone can be affected by its properties.

Output signal from the input buffer is then converted into a differential form to improve noise immunity and consequently, the differential signal is amplified. Since the low corner frequency of the RI is set to 30Hz, two external (off-chip) capacitors (with capacitance in order of hundreds of nF) are employed to implement the high-pass filter (HPF) with the slope of 20 dB per decade. The active low-pass filter (LPF) with the slope of 40 dB/decade is realized completely on a chip. Consequently, the output signal from the LPF is buffered and processed by the sigma-delta modulator.

### 3.2. Input conversion block

The most important building block of the proposed RI is the input conversion block. Its main role is to convert the capacitance variations into voltage changes. Transistor level schematic of the designed input conversion block as well as size of the transistors used in the input buffer are depicted in Fig. 2.

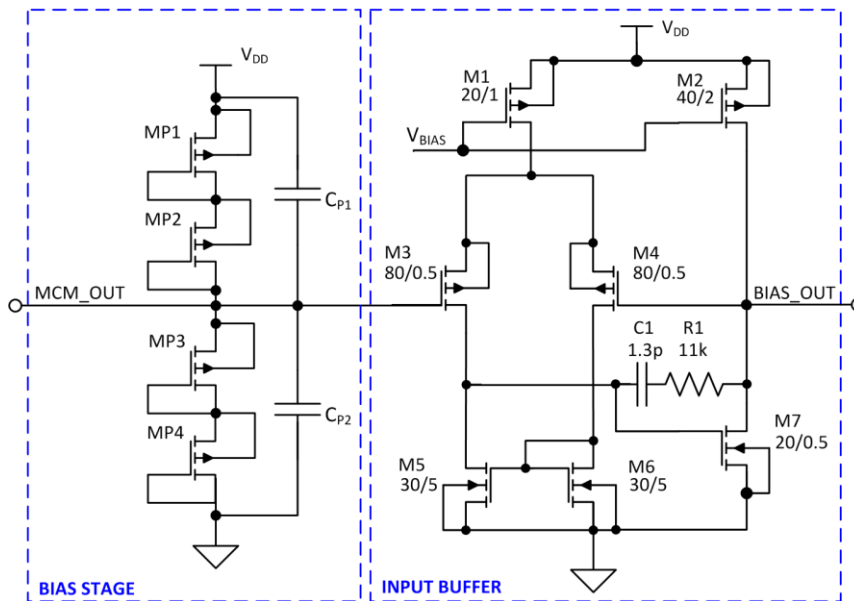


Fig. 2 Schematic diagram of the input conversion block

The proposed readout approach is based on the buffered input conversion stage, where the main challenge is how to ensure the DC bias voltage for the input buffer. Since the output impedance of the MCM is very high, another important task is to maintain the input impedance of the input conversion block as higher as possible. In order to achieve high input impedance of the input conversion block, in our case, the DC bias voltage was

provided by a voltage divider implemented with diode-connected MOS transistors. This represents rather important advantage of the proposed readout approach. To achieve a high resistance of the MOS transistor,  $W/L$  ratio should be lower than 1.

The main requirement for the input buffer is low voltage noise and low value of the input offset. However, a two-stage OPAMP topology has been used for realization of the input LNA buffer (Fig. 2). In order to increase common-mode input range, bulk of the MOS transistors used in the input differential pair was shorted with source. In this way, the body effect of those transistors is eliminated. Bias voltage ( $V_{BIAS}$ ) is generated on chip using a mirrored reference current. Design of the LNA buffer has been optimized by the proper transistor size to obtain low noise and low input offset voltage. Nevertheless, from the whole readout frontend circuit point of view, the input offset voltage of LNA is not critical parameter because DC voltage is removed by external coupling capacitors C1 and C2 (Fig. 1). Since the input capacitance of the input buffer depends on gate-source capacitance ( $C_{GS}$ ) of input transistors used in the buffer, sizes of the input transistors have to be optimized in order to reduce capacitance  $C_{GS}$ . To reduce the input noise caused by the MCM, capacitors  $C_{P1}$  and  $C_{P2}$  were connected in parallel with the diode-connected MOS transistors (Fig. 3). On the other hand, capacitances  $C_{P1}$  and  $C_{P2}$  together with capacitance of the microphone form a capacitive divider (sensitivity of the MCM might be influenced). Therefore, another critical issue is minimization of the impact of capacitances  $C_{P1}$  and  $C_{P2}$ , which can negatively affect the microphone sensitivity.

Small-signal equivalent circuit of the input conversion block is depicted in Fig. 3, where  $C_{MCM}$  is the nominal capacitance of the microphone,  $C_{in\_buff}$  is the input capacitance of the input buffer and  $r_{DS}$  represents a resistance of the respective diode-connected MOS transistor.

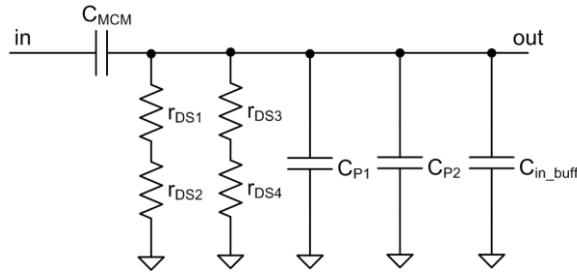


**Fig. 3** Small-signal equivalent circuit of the input conversion block

Transfer function of the proposed block is expressed by Eq. 1.

$$A(s) = \frac{C_{MCM}}{C_{MCM} + C_{TOT}} \times \frac{1}{1 + \frac{C_{MCM}}{C_{MCM} + C_{TOT}} \times \frac{1}{sC_{MCM}r_{DS}}} \quad (1)$$

Capacitance  $C_{TOT}$  represents the sum of capacitances  $C_{P1}$ ,  $C_{P2}$  and  $C_{in\_buff}$ . However, transfer function can be rewritten as:

$$A(s) = k \times \frac{1}{1 + k \times \frac{1}{s C_{MCM} r_{DS}}} \quad (2)$$

where

$$k = \frac{C_{MCM}}{C_{MCM} + C_{TOT}} \quad (3)$$

From transfer function, one can express the gain and corner frequency of the inverted pole. As can be seen from Eq. 2, gain of the transfer function is multiplied by term  $k$ . Thus, sensitivity of the microphone depends on the ratio of capacitances  $C_{MCM}$  and  $C_{TOT}$ , expressed by Eq. 3. Hence, in terms of requirements for the MCM sensitivity, values of capacitors  $C_{P1}$  and  $C_{P2}$  should be at least 10 times lower than the nominal capacitance ( $C_{MCM}$ ) of the microphone. Under this condition, the original value of the MCM sensitivity is maintained.

The low frequency corner, formed by the input conversion block, can be expressed as:

$$f_{L-3dB} = \frac{1}{2\pi r_{DS} (C_{MCM} + C_{TOT})} \quad (4)$$

From Eq. 4, one can observe that capacitors  $C_{P1}$  and  $C_{P2}$  might cause an undesired shift of the low corner frequency of the readout interface. Therefore, to maintain the original value of the low corner frequency, the values of capacitors  $C_{P1}$  and  $C_{P2}$  should be chosen appropriately. To conclude, we would like to underline that capacitors  $C_{P1}$  and  $C_{P2}$  can be used for noise reduction but in order to maintain the original value of the MCM sensitivity and low corner frequency of the readout circuit, their values must be carefully selected.

#### 4. RESULTS AND DISCUSSION

For evaluation the designed RI, the main parameters were simulated in Cadence design environment. Fig. 4 shows the boundary frequency responses of the proposed readout circuit obtained from Corner Analysis, where the process and temperature variations were taken into account. The low corner frequency will vary from 19.2 Hz to 33.1 Hz while the high corner frequency is kept in the range from 7.4 kHz to 15.2 kHz. The obtained gain is in the range from 24.6 dB to 26.1 dB. Slope of the LPF and HPF is 10dB/octave and 18dB/octave, respectively. However, shape of the final frequency response mainly depends on the frequency response of the MEMS microphone itself.

Further parameter that expresses the linearity of the RI circuit is the Total Harmonic Distortion (THD), which depends on the amplitude of the input signal. Fig. 5 shows the dependence of the THD parameter on the input amplitude. It can be observed that THD will be lower than 0.1% for the input amplitude in the range from 100  $\mu$ V to 70 mV. For the input amplitude over 70 mV, the THD will rapidly increase, and as the input amplitude reaches 100 mV the THD of whole RI will be about 0.6%.

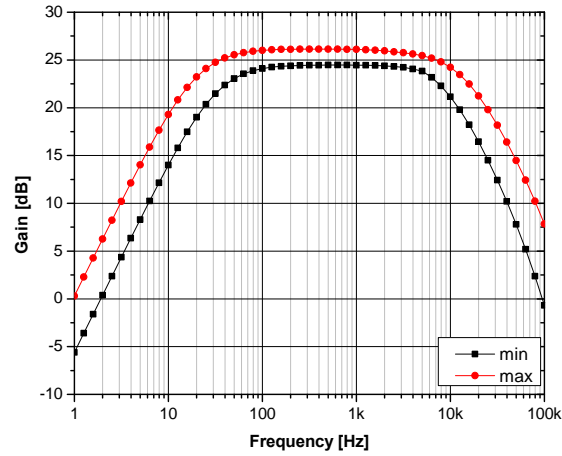


**Fig. 4** Frequency response of the RI circuit

The linearity of the RI can also be observed from Fig. 5, where the dependence of the output amplitude on the input amplitude is shown. Since the input range of the sigma-delta modulator is from 0 V to 2 V, one can observe that in the whole considered range, the proposed RI exhibits good linearity.

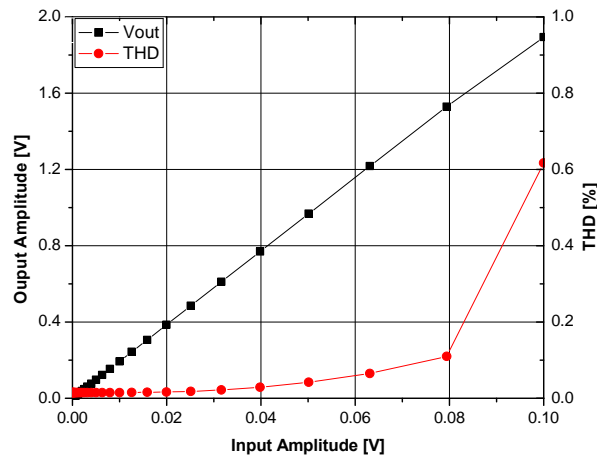


**Fig. 5** Output amplitude and THD versus the input amplitude

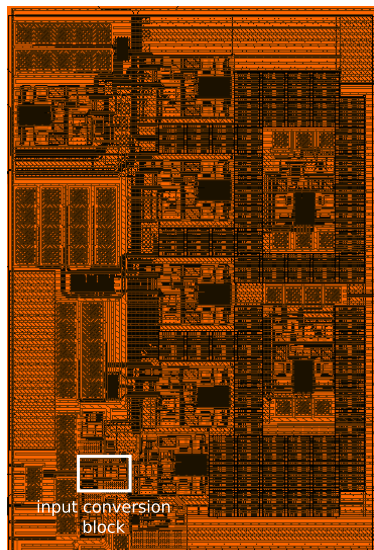
The main achieved parameters of the designed readoutfrontend circuit obtained from schematic as well as postlayout simulations are summarized in Tab. 1. Layout of the proposed readout frontend circuit and comparison of the frequency responses obtained from schematic and postlayout simulations are depicted in Fig. 6a and Fig. 6b, respectively. In Fig. 6a, the input conversion block is marked. From Tab. 1 and Fig. 6b, one can observe that the biggest change in the frequency response was achieved at higher



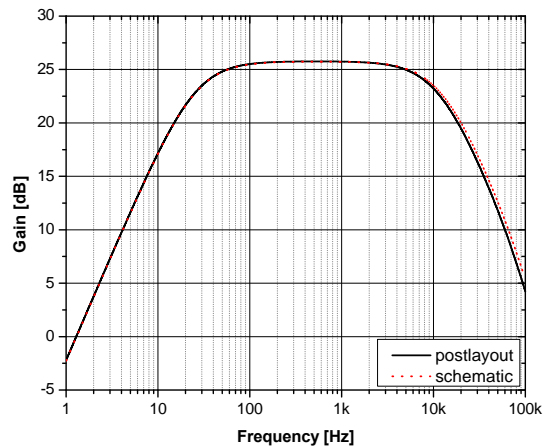
frequencies. The high frequency corner 9.66 kHz was achieved, which represents about 10% lower value compared to the schematic simulation result. Other parameters either slightly change or maintain their original values.

**Table 1** Main parameters of the proposed readout frontend circuit

| Parameter                              | Conditions                   | Typical | Postlayout | Unit                           |
|--|------------------------------|---------|------------|--------------------------------|
| Maximum Gain                           |                              | 25.75   | 25.7       | dB                             |
| Frequency Response                     | Low frequency -3 dB point    | 25.75   | 25.6       | Hz                             |
|  | High frequency -3 dB point   | 10.66   | 9.66       | kHz                            |
| Noise                                  | Input noise @ 1 kHz          | 0.293   | 0.27       | $\mu\text{V}/\sqrt{\text{Hz}}$ |
|  | Output noise @ 1 kHz         | 5.66    | 5.24       | $\mu\text{V}/\sqrt{\text{Hz}}$ |
| THD                                    |                              | 0.099   | 0.096      | %                              |
| Signal to Noise (S/N)                  |                              | 68.76   | 68.31      | dB                             |
| Dynamic Range (DR)                     |                              | 110.6   | 110.7      | dB                             |
| $I_{DD}$ consumption of selected block | Input conversion block       | 50      | 50         | $\mu\text{A}$                  |
|  | Single-ended to differential | 165     | 165        | $\mu\text{A}$                  |
|  | 2x AMP                       | 550     | 550        | $\mu\text{A}$                  |
|  | Filter                       | 820     | 820        | $\mu\text{A}$                  |
| Total $I_{DD}$ consumption             | $V_{DD} = 3\text{V}$         | 1.56    | 1.56       | mA                             |



a) Layout of the readout frontend



b) Postlayout vs schematic simulation results

**Fig. 6** RI layout and post-layout simulation results

Comparison of the achieved results to other works is presented in Tab.2.

**Table 2** Comparison of the achieved results

|                                       | [27]                        | [29]                  | [30]               | [31]                                   | this work                             |
|---------------------------------------|-----------------------------|-----------------------|--------------------|--|---------------------------------------|
| CMOS Process                          | 0.35 $\mu\text{m}$          | 0.35 $\mu\text{m}$    | 0.8 $\mu\text{m}$  | 0.8 $\mu\text{m}$                      | 0.35 $\mu\text{m}$                    |
| Supply                                | $\pm 1.65$ V                | 3.3 V                 | 5 V                | 5 V                                    | 3 V                                   |
| Power                                 | 7.9 mW                      | N/A                   | 8.38 mW            | 0.56 mW                                | 4.68 mW                               |
| Area                                  | 0.24 $\text{mm}^2$          | 12 $\text{mm}^2$      | 1.21 $\text{mm}^2$ | 0.22 $\text{mm}^2$                     | 0.29 $\text{mm}^2$                    |
| Peak SNDR/DR                          | 91.7 dB                     | N/A                   | 60 dB              | N/A                                    | 110.66 dB                             |
| Noise Floor                           | N/A                         | N/A                   | N/A                | 0.25 aF/ $\sqrt{\text{Hz}}$<br>(500Hz) | 0.09 aF/ $\sqrt{\text{Hz}}$<br>(1kHz) |
| Adjustable Gain<br>(by drive current) | yes                         | no                    | no                 | no                                     | no                                    |
| Sensitivity                           | 0.1 V <sub>norm</sub> /1pF  | 38 $\mu\text{sec/pF}$ | 9980 mV/fF         | 12.42 mV/fF                            | 62.6 mV/fF                            |
| Output Swing                          | N/A                         | N/A                   | N/A                | N/A                                    | SE: 1.9 V<br>DE: 3.8 V                |
| Approach                              | CV with AC<br>drive current | Semi-digital<br>(PWM) | SC                 | SC                                     | CC                                    |

SC - switching capacitors, SE: single ended, DE: differential ended,  
DR: dynamic range, CV: constant voltage, CC: constant charge

Nevertheless, it is important to note that the other works are based on different approaches, so the comparison might not be fully relevant. Thus, we also specify the approach, which the respective design is employing. As can be observed, in our case, the best result was achieved for the dynamic range (DR) parameter, where 110dB is achieved as required by the target application. Moreover, sensitivity and input noise as well as the noise floor obtained by this approach are better than those presented in [31]. The proposed readout circuit requires smaller chip area than in approaches presented in [29] and [30] by 18% and 23% higher than [27] and [31], respectively. Finally, in comparison to other works, the most important improvements and features of the presented readout frontend circuitry can be summarized as follows:

- broader dynamic range
- better noise performance
- low power consumption

However, these features are achieved at costs of area overhead (about 20% with respect to works presented in [27] and [31]).

## 5. CONCLUSION

The frontend part of the readout interface for MCM was proposed and designed in a standard 0.35  $\mu\text{m}$  CMOS technology. The achieved results show that the proposed approach brings the high dynamic range and very good noise performance, which are the most important parameters required by a MCM-based noise dosimeter meant to be used in very harsh environment.

Currently, the developed readout interface is being fabricated. In the future research, evaluation of prototype chips will be performed and possible modification of the RI design towards further improvements is expected.

**Acknowledgement.** *This work was supported in part by the EC under FP7 ICT Project SMAC (288827), ENIAC JU under Project E2SG (296131), and by the Slovak Republic under grant VEGA 1/0823/13.*

#### REFERENCES

- [1] G. W. Elko, F. Pardo, D. Lpez, D. Bishop, and P. Gammel, "Capacitive MEMS microphones", *Bell Labs Technical Journal*, vol. 10, no. 3, pp. 187–198, 2005.
- [2] S. A. Jawed, D. Cattin, M. Gottardi, N. Massari, R. Oboe, and A. Baschiroto, "A low-power interface for the readout and motion-control of a MEMS capacitive sensor", In 10th IEEE International Workshop on Advanced Motion Control, AMC 2008, pp. 122–125.
- [3] C.-T. Chiang, W.-C. Chou, J.-C. Tsai, and H.-L. Lee, "ACMOS readout circuit with frequency optimization for microphone sensor arrays", In Proceedings of the International Symposium on Computer Communication Control and Automation, 3CA 2010, vol. 2, pp. 249–252.
- [4] J.-T. Huang, K.-S. Chen, and C.-C. Chien, "A differential capacitive sensing circuit for micro-machined omnidirectional microphone", In Proceedings of the IEEE International Conference on Nano/Micro Engineered and Molecular Systems, NEMS 2011, pp. 948–951.
- [5] J. van den Boom, "A 50\_W biasing feedback loop with 6mssettling time for a MEMS microphone with digital output", In Digest of Technical Papers the IEEE International Solid-State Circuits Conference, ISSCC 2012, 2012, pp. 200–202.
- [6] Brüel and Kjaer, "Microphone Handbook", vol. 1 Theory. Nearum, Denmark: Brüel and Kjaer, 1996.
- [7] Tao Yin; Huanming Wu; Qisong Wu; Haigang Yang; Jiao, J., "A TIA-based readout circuit with temperature compensation for MEMS capacitive gyroscope", In Proceedings on IEEE International Conference on Nano/Micro Engineered and Molecular Systems, NEMS 2011, pp. 401–405, 20-23 Feb. 2011.
- [8] Jawed, S. A; Gottardi, M.; Baschiroto, A, "A Switched Capacitor Interface for a Capacitive Microphone," *Research in Microelectronics and Electronics 2006*, Ph. D., pp. 385-388.
- [9] Sheng-Yu Peng; Qureshi, M.S.; Hasler, P.E.; Basu, A; Degertekin, F.L., "A Charge-Based Low-Power High-SNR Capacitive Sensing Interface Circuit," *IEEE Transactions on Circuits and Systems I: Regular Papers*, vol.55, no.7, pp.1863–1872, Aug. 2008.
- [10] W. Jiangfeng, G.K. Fedder, L.R. Carley, "A low-noise low-offset capacitive sensing amplifier for a 50- $\mu\text{g}/\sqrt{\text{Hz}}$  monolithic CMOS MEMS accelerometer," *IEEE Journal of Solid-State Circuits*, vol.39, no.5, pp. 722–730, May 2004.
- [11] Pastre, M., Kayal, M. *Methodology for the Digital Calibration of Analog Circuits and Systems: With Case Studies*, 1st ed. Springer Publishing Company, Incorporated, 2009.
- [12] A. van Roermund, A. Baschiroto, and M. Steyaert, *Nyquist AD Converters, Sensor Interfaces, and Robustness: Advances in Analog Circuit Design*, 2012, ser. Springer Link: Bücher. Springer, 2012.
- [13] L. Baxter, *Capacitive Sensors: Design and Applications*, ser. IEEE Press Series on Electronics Technology. John Wiley & Sons, 1996.
- [14] S. A. Jawed, D. Cattin, M. Gottardi, N. Massari, A. Baschiroto, and A. Simoni, "A 828 $\mu\text{W}$  1.8V 80dB dynamic-range readout interface for a MEMS capacitive microphone", In Proceedings on 34th European Solid-State Circuits Conference, ESSCIRC 2008, Sept 2008, pp. 442–445.
- [15] I. Deligoz, S. Naqvi, T. Copani, S. Kiaei, B. Bakkaloglu, S.-S. Je, and J. Chae, "A MEMS-Based Power-Scalable Hearing Aid Analog Front End", *IEEE Transactions on Biomedical Circuits and Systems*, vol. 5, no. 3, pp. 201–213, June 2011.
- [16] S. A. Jawed, J. Nielsen, M. Gottardi, A. Baschiroto, and E. Bruun, "A multifunction low-power preamplifier for MEMS capacitive microphones", In Proceedings of ESSCIRC, ESSCIRC 2009, Sept 2009, pp. 292–295.
- [17] C. Furst, "A low-noise/low-power preamplifier for capacitive microphones", In Proceedings on the IEEE International Symposium on Circuits and Systems Connecting the World, ISCAS 1996, vol. 1, May 1996, pp. 477–480.

- [18] C. Enz, E. Vittoz, F. Krummenacher, "A CMOS chopper amplifier", *IEEE Journal Solid-State Circuits*, vol. 22, no. 3, Jun 1987, p. 335–342.
- [19] C. Enz, and G. Temes, "Circuit techniques for reducing the effects of op-amp imperfections: autozeroing, correlated double sampling, and chopper stabilization", In Proceedings of the IEEE, vol. 84, no. 11, Nov 1996, pp. 1584–1614.
- [20] M. White, D. Lampe, F. Blaha, I. Mack, "Characterization of surface channel CCD image arrays at low light levels", *IEEE Journal Solid-State Circuits*, vol. 9, no. 1, Feb 1974, pp. 1–12.
- [21] M. Pederson, W. Olthuis, P. Bergveld, "High-performance condenser microphone with fully integrated CMOS amplifier and DC-DC voltage converter," *Journal of Microelectromechanical Systems*, vol.7, no.4, pp. 387–394, Dec 1998.
- [22] C. E. Furst, "A low-noise/low-power preamplifier for capacitive microphones," In Proceedings on the IEEE International Symposium on Circuits and Systems Connecting the World, ISCAS 1996, 12-15 May 1996, vol. 1, pp. 477–480.
- [23] S. A. Jawed, D. Cattin, N. Massari, M. Gottardi, and A. Baschirotto, "A MEMS microphone interface with force-balancing and charge-control", in Research in Microelectronics and Electronics, 2008. PRIME 2008. Ph.D., June 2008, pp. 97–100.
- [24] T. ting Zhang, H.-J. Li, J.-Q. Huang, M. Zhao, L.-C. Hong, Y.-C. Zhang, W.-G. Lu, and Z.-J. Chen, "An offset-compensated switched-capacitor interface circuit for closed-loop MEMS capacitive accelerometer", In Proceedings on the IEEE 11th International Conference on Solid-State and Integrated Circuit Technology, ICSICT 2012, Oct 2012, pp. 1–3.
- [25] L. Dong-Hyuk, L. Sang-Yoon, C. Woo-Seok, P. Jun-Eun, and D.-K. J., "A Digital Readout IC with Digital Offset Canceller for Capacitive Sensors", *Journal of Semiconductor Technology and Science*, vol. 12, no. 3, pp. 278–285, 2012.
- [26] B. Fowler, M. Godfrey, and S. Mims, "Reset noise reduction in capacitive sensors", *IEEE Transactions on Circuits and Systems I: Regular Papers*, vol. 53, no. 8, pp. 1658–1669, Aug 2006.
- [27] F. Aezinia and B. Bahreyni, "A readout circuit with wide dynamic range for differential capacitive sensing applications", In Proceedings 26th Annual IEEE Canadian Conference on Electrical and Computer Engineering, CCECE 2013, May 2013, pp. 1–4.
- [28] J.-L. Lu, M. Inerowicz, S. Joo, J.-K. Kwon, and B. Jung, "A Low-Power, Wide-Dynamic-Range Semi-Digital Universal Sensor Readout Circuit Using Pulsewidth Modulation", *IEEE Sensors Journal*, vol. 11, no. 5, pp. 1134–1144, May 2011.
- [29] M. Lee, S. Lee, S. Jung, C. Je, G. Hwang, and C. Choi, "Design, Fabrication, and Characterization of a Readout Integrated Circuit (ROIC) for Capacitive MEMS Sensors", *Sensors*, 2007 IEEE, pp. 260–263. Oct 2007.
- [30] J. Shiah, H. Rashtian, and S. Mirabbasi, "A low-noise parasitic-insensitive switched-capacitor CMOS interface circuit for MEMS capacitive sensors", In Proceedings on the IEEE 9th International New Circuits and Systems Conference, NEWCAS 2011, June 2011, pp. 470–473.
- [31] J. Shiah and S. Mirabbasi, "A 5-V 555- $\mu$ W 0.8- $\mu$ m CMOS MEMS capacitive sensor interface using correlated level shifting", In Proceedings on the IEEE International Symposium on Circuits and Systems, ISCAS 2013, May 2013, pp. 1504–1507.